ACS OMEGA

http://pubs.acs.org/journal/acsodf

Article

Complexation of an Azo Dye by Cyclodextrins: A Potential Strategy for Water Purification

Anas Saifi, Jojo P. Joseph, Atul Pratap Singh, Asish Pal, and Kamlesh Kumar*

Cite This: *ACS Omega* 2021, 6, 4776−4782

Read Online

ACCESS | Metrics & More | Article Recommendations | Supporting Information

ABSTRACT: The chemistry of the host−guest complex formation has received much attention as a highly efficient approach for use to develop economical adsorbents for water purification. In the present study, the synthesis of three β-cyclodextrin (β-CD) inclusion complexes with the oil orange SS (OOSS) azo dye as a guest molecule and their potential applications in water purification are described. The complexes were synthesized by the coprecipitation method and characterized by Fourier transform infrared (FTIR) spectroscopy, UV−vis spectroscopy, X-ray diffraction (XRD), thermogravimetric analysis (TGA), and differential scanning calorimetry (DSC). FTIR and thermal analyses confirmed the encapsulation of OOSS dye within the hydrophobic cavity of β-CD. The encapsulation of hydrophobic dye inside the β-CD cavity was mainly due to the hydrophobic−hydrophobic interaction. The results showed that the stability of the OOSS dye had been improved after the complexation. The effect of three different compositions of the host−guest complexes was analyzed. The present study demonstrated that the hydrophobic dye could be removed from aqueous solution via inclusion complex formation. Thus, it can play a significant role in removing the highly toxic OOSS dye from the industrial effluent.

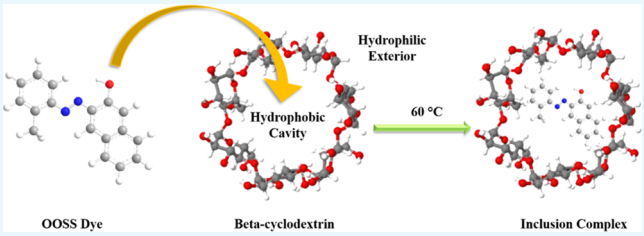

1. INTRODUCTION

Many industries, in particular textile and printing, use synthetic organic compounds such as dyes as an essential category of materials.[1−4] According to their chemical structure, dyes may be classified as azo, cyanine, anthraquinone, carbonyl, nitro, sulfur, styryl, or phthalocyanine dyes.[5] Nowadays, azo dyes are commonly utilized in various industries such as textile, food colorants, printing, and cosmetics. Approximately, 30−70% of the total azo dye produced is released into the atmosphere, primarily via wastewater, and its degradation products affect living organisms as they are toxic and carcinogenic in nature.[6−9]

The oil orange SS (OOSS) dye is one of the azo compounds, a possible human carcinogen, and is classified as group 2B compounds by the International Agency for Research on Cancer (IARC). The OOSS dye is generally used as a color toner in the printing industry and discharged into water during synthesis and printing processes, leading to water pollution.[10] Due to the presence of large degree of aromatic compounds in the OOSS dye, it is essential to treat OOSS dye-containing wastewater before discharge. Various physical and chemical methods are currently utilized for dye removal by conventional technologies, for instance, adsorption, ultrafiltration, coagulation, electrochemical degradation, photocatalysis, etc.[11−16] However, due to its simplicity and requirement of less energy, adsorption is one of the most effective and common methods among the various reported techniques. In this context, supramolecular chemistry offers crucial routes for the preparation of different adsorbents and extraction reagents.[7] This is achieved by introducing macrocyclic receptors, such as crown ethers,[17] calixarenes,[18] and cyclodextrins,[19] which provide suitable binding sites.

β-Cyclodextrin (β-CD) is a naturally occurring cyclic oligosaccharide with a torus structure. It comprises seven α-1,4-linked-glucopyranose units consisting of an interior hydrophobic cavity and exterior hydrophilic surface.[20] The most important feature of the β-CD structural composition is the formation of inclusion complexes with various aromatic compounds, including dyes, through host−guest interactions[21−26] via hydrophobic−hydrophobic interactions.[27] These kinds of host−guest inclusion complexes can be used in drug delivery,[28] cosmetics,[29] and water purification applications.[30]

β-CD and its derivatives have been extensively studied in removing metals,[31] organic dyes,[32,33] and other water micropollutants.[34,35] Among the transition metal ions, the adsorption of transition metal ions like Pb has been commonly reported with different derivatives of β-CD. Similarly, among the different supramolecular macrocycles, extensive research has been conducted for dye adsorption with β-CD. Recently,

Received: November 23, 2020
Accepted: January 27, 2021
Published: February 5, 2021

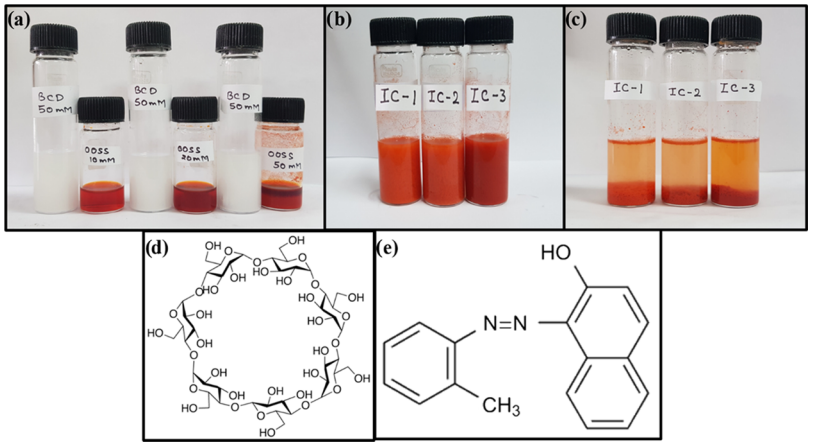

Figure 1. (a) Aqueous solution of 50 mM β-CD in 10 mL of DI water and 2, 5, and 10 mM OOSS dye in 4 mL of ethanol; (b) after mixing both solutions at room temperature; (c) inclusion complexes between β-CD and the OOSS dye of three different compositions; (d) chemical structure of β-CD; and (e) chemical structure of the OOSS dye.

Nasiri et al. reported iron-based nanoadsorbents for crystal violet (CV) dye adsorption.[36] Fan et al. reported the removal of methylene blue dye by β-CD-modified Fe_3O_4 nanoparticles and its reaction with chitosan.[37] The β-CD-based adsorbent reported by Crini et al. exhibited high adsorption capacities toward Basic Blue 9.[38] Zhao et al. reported five times reusability with high-separation-efficiency β-CD-based fibers for methylene blue.[39] Several authors also reported that β-CD could be used as a multiadsorbent. Duan et al. reported CD-based polymers, which can specifically remove pollutants in fuel and methylene blue in the effluent.[40] Chen et al. reported a one-step treatment for the removal of methyl orange and Pb(II) using β-CD- and polyethyleneimine (PEI)-functionalized magnetic nanoadsorbents.[41] Qin et al. also reported a "pocket" structure that shows excellent adsorption for the simultaneous removal of organic dyes (rhodamine B and Congo red) and heavy metal ions Cd(II) via a β-CD-crosslinked polymer.[42]

In the present study, we focused on preparing the β-CD inclusion complex with the hydrophobic OOSS dye via the coprecipitation method. Moreover, we explored the effect of OOSS dye concentration on complexation of the synthesized material and the competitive behavior of the OOSS dye with the hydrophilic crystal violet dye for encapsulation into the β-CD cavity. To the best of our knowledge, no previous study has been conducted on OOSS dye inclusion complex formation. The reported strategy has a potential application in removing toxic dyes and wastewater purification.

2. EXPERIMENTAL SECTION

2.1. Reagents. β-CD (Sisco Research Laboratories Pvt., Ltd.) and OOSS dye (Tokyo Chemical Industries) were used as received without further purification. Ethanol was received from Sigma-Aldrich. Deionized (DI) water was used throughout the experiments to prepare the solutions.

2.2. Synthesis of β-CD−OOSS Dye Inclusion Complexes. The inclusion complexes of β-CD and OOSS dye were synthesized by the coprecipitation method. The solutions of β-CD were prepared in a glass vial by dissolving 50 mM β-CD in 10 mL of DI water at 60 °C. For investigating the effect of the host−guest composition, different concentrations of the OOSS dye, 1, 2, and 5 mM, in 4 mL of ethanol were chosen for preparing IC-1, IC-2, and IC-3, respectively. The OOSS dye solution was added dropwise to the β-CD solution, and the suspension was kept for continuous stirring at room temperature (RT). The solution was then heated overnight at 60 °C without stirring, and the suspension was allowed to precipitate. The solution was centrifuged at 9000 rpm for 15 min, washed a couple of times with DI water, freeze-dried for 6 h, and stored at room temperature for further characterization. A similar strategy was utilized to synthesize a competitive inclusion complex of β-CD with the hydrophobic OOSS dye and hydrophilic crystal violet dye.

2.3. Characterization. The Fourier transform infrared (FTIR) spectra were obtained in the 400−4000 cm^{-1} range using Nicolet iS10 and using KBr as a pellet. UV−vis measurements were carried out with a Cary 4000 UV−vis double-beam spectrophotometer. Thermal analysis by thermogravimetric analysis (TGA) was performed in the Shimadzu DTG-60H apparatus using a TA-60WS thermal analyzer from 30 to 500 °C at a rate of 10 °C/min. Differential scanning calorimetry (DSC) was recorded on a PerkinElmer differential scanning calorimeter, DSC 8000 model, and the samples were heated from 20 to 180 °C at a heating rate of 10 °C/min under a nitrogen atmosphere. XRD spectra were recorded using a Bruker D8 advance powder X-ray diffractometer operated at 20 mA current and 40 kV using a Cu Kα source with a wavelength of 1.54 Å.

3. RESULTS AND DISCUSSION

The coprecipitation method has been exploited to accomplish the inclusion complex formation of the β-CD−OOSS dye. The OOSS dye is a hydrophobic azo dye, and it can be encapsulated into the hydrophobic cavity of the β-CD via the hydrophobic−hydrophobic interactions. For the inclusion complex synthesis, different predetermined molar solutions of β-CD and OOSS dye were prepared in DI and ethanol, respectively, as shown in Figure 1a. The OOSS dye solutions were then added dropwise to the aqueous solutions of β-CD with continuous stirring, Figure 1b. The solutions were heated at 60 °C overnight, and the suspension was allowed to precipitate at room temperature, Figure 1c. To remove unreacted moieties, the solutions were centrifuged and filtrates were washed with water. Afterward, the precipitate was freeze-dried to obtain the inclusion complex and stored at room temperature.

https://dx.doi.org/10.1021/acsomega.0c05684
ACS Omega 2021, 6, 4776−4782

The optical images show that using this coprecipitation method, the toxic OOSS dye can be easily adsorbed from the industrial effluent via the formation of an inclusion complex between β-CD and the OOSS dye. Moreover, we analyzed similar results of the adsorption of OOSS dye by β-CD in textile industrial waste and lake water as shown in Figure S1. Therefore, β-CD can play a significant role in water purification in terms of removal of toxic dyes from wastewater.

FTIR provides the structural information of β-CD and the OOSS dye that can be used to estimate the interactions between the host and guest molecule. In Figure 2a, the β-CD spectrum presents broad characteristic peaks at 3390 cm^{-1} (O−H stretching), 2920 cm^{-1} (C−H stretching in the pyranoid ring), 1639 cm^{-1} (C═O stretching), 1380 cm^{-1} (C−H bending), 1160 cm^{-1} (asymmetric stretching of the glycosidic C−O−C bridge), and 1030 cm^{-1} (CH_2−OH vibration).[43,44] Figure 2b shows the OOSS dye spectrum, which exhibits characteristic peaks at 3450 cm^{-1} (−OH stretching), 3062 cm^{-1} (C−H stretching), 1400−1500 and 1585−1600 cm^{-1} (C−C stretching vibrations in the aromatic ring), and 1000−1250 cm^{-1} (C−H in-plane bending). Figure 2c−e shows main absorption patterns of the inclusion complexes, which comprise characteristic peaks ascribed to β-CD and the OOSS dye and exhibit slight changes in the frequency of a functional group of the inclusion complex due to the van der Waals interaction, which is attributed to the formation of the inclusion complex.[45]

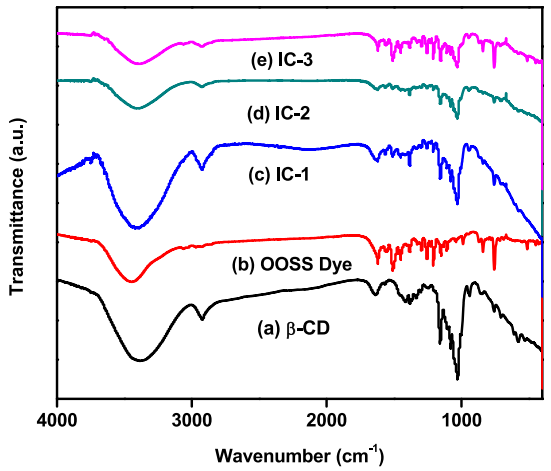

Figure 2. FTIR spectra of (a) β-CD, (b) OOSS dye, (c) IC-1, (d) IC-2, and (e) IC-3.

The FTIR spectra of inclusion complexes exhibit slight changes where −OH stretching occur at ∼3400 cm^{-1} becomes narrower, CH_2 stretching at 2930 cm^{-1}, C═O stretching at 1630 cm^{-1}, of β-CD and consists of C−C stretching vibrations of OOSS dye. It was also noted that on increasing the concentration of OOSS dye, i.e., IC-1, IC-2, and IC-3, it exhibited relatively lower intensity characteristic peaks than the pure β-CD and OOSS dye. Inclusion complexes displayed greater resemblance to the β-CD spectrum rather than OOSS dye, which showed that the OOSS dye was encapsulated in the cavity of β-CD.[46] The frequency of functional groups increased because of the location of the azo dye through the electron-rich cavity of β-CD and decreased due to the reaction of van der Waals forces and hydrogen bonding during the formation of the inclusion complex.[47,48] The significant differences in C−H and C═O vibration modes and narrowing of the −OH functional group at ∼3400 cm^{-1} were indicative of the formation of inclusion complexes. These results are in agreement with previously reported inclusion complexes.[49,50]

The formation of the inclusion complex between β-CD and the OOSS dye is confirmed by absorption spectra, as shown in Figure 3(i). It was found that β-CD had no absorption peak,[51−53] while the OOSS dye showed two absorption peaks, i.e., at 314 and 494 nm, which were due to the $\pi-\pi^*$ and $n-\pi^*$ transitions, respectively. In the case of $\pi-\pi^*$ transition, a hypsochromic shift was observed in IC-1 and IC-2 as there was a change in the position of λ_{max} to a shorter wavelength, i.e., 312 nm, compared to the pure OOSS dye, i.e., 314 nm. This shift occurred due to change in polarity, which was attributed to the fact that the less polar OOSS dye was present in the more polar β-CD cavity.[54] A significant hyperchromic shift can be seen from IC-1 to IC-2, as shown in Figure 3(ii), as a higher

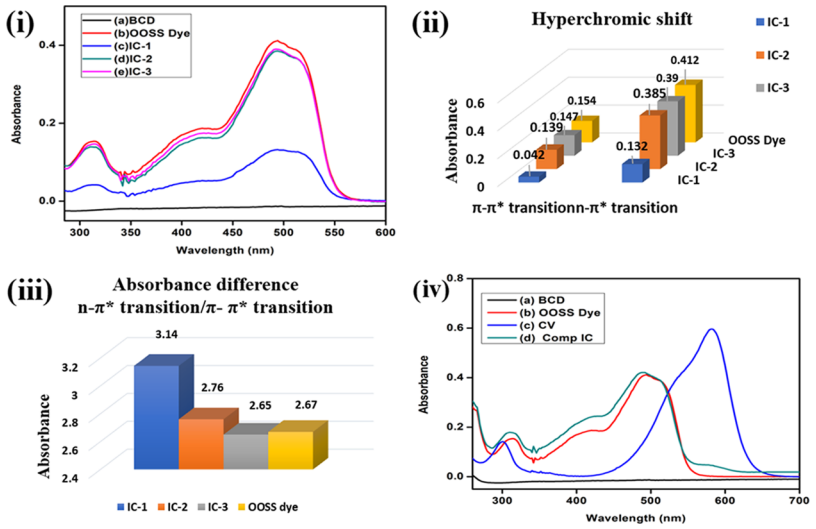

Figure 3. (i) Absorption spectra of (a) β-CD, (b) OOSS dye, (c) IC-1, (d) IC-2, and (e) IC-3. (ii) Hyperchromic shift as a function of concentration. (iii) Absorbance difference between two different transitions states. (iv) Absorption spectra of competitive spectra of the OOSS dye and crystal violet (CV) dye.

https://dx.doi.org/10.1021/acsomega.0c05684
ACS Omega 2021, 6, 4776−4782

amount of OOSS dye was present in the hydrophobic cavity of β-CD, which indicates the inclusion complex formation.

In the case of the n−π* transition, a hypsochromic shift was observed from IC-2 (494 nm) to IC-3 (492 nm) and a slight hyperchromic shift was observed from IC-2 to IC-3, while the hyperchromic shift from IC-1 to IC-2 was very significant as a function of concentration, Figure 3(ii). Also, the difference between the absorbance intensities of both peaks, i.e., π−π* and n−π*, as shown in Figure 3(iii), was also observed in the inclusion complexes, and it was found to be decreasing as a function of concentration. Therefore, these facts indicate the inclusion complex formation.

We also investigated the competitive behavior of the hydrophobic OOSS dye in the β-CD inclusion complex by UV−vis spectroscopy. The absorption spectra in Figure 3(iv) displayed that the hydrophobic OOSS dye has a greater affinity for the β-CD cavity instead of the hydrophilic crystal violet (CV) dye. In the case of competitive IC, no peak of the crystal violet dye was observed, while absorbance spectra were similar to those of the inclusion complex of the OOSS dye.

The stability of the complexes was analyzed by thermogravimetric analysis and is displayed in Figure 4. The thermogram

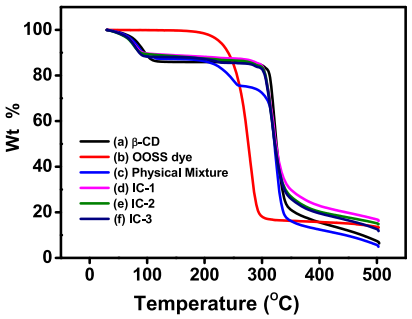

Figure 4. Thermogravimetric analysis (TGA) thermograms of (a) β-CD, (b) OOSS dye, (c) physical mixture, (d) IC-1, (e) IC-2, and (f) IC-3.

of β-CD showed the mass loss in two stages. In Figure 4a, in the first stage, ∼14% weight loss occurred at ∼110 °C, which is related to dehydration, whereas ∼75% weight loss occurs at ∼340 °C in the later stage, which is associated with the decomposition of the macrocycles.[55] However, in Figure 4b, the OOSS dye exhibited a weight loss of 84% at ∼290 °C, which is due to the degradation of the organic compounds. The curve of the physical mixture shows the superposition of β-CD and OOSS dye, with 12% initial mass loss, and 25 and 84% of its mass loss occur at ∼260 and ∼340 °C due to degradation of the OOSS dye and β-CD macrocycle, respectively, as shown in Figure 4c. The inclusion complexes underwent weight losses in two stages, which confirmed the inclusion of OOSS dye inside the β-CD. The inclusion complexes (IC-1, IC-2, and IC-3) showed lower degradation at the first stage because of the incorporation of OOSS dye inside the cavity of β-CD replacing water molecules when compared to pure β-CD and the physical mixture.[56] However, at the second stage, they show almost 15−17% less weight loss at the same temperature, i.e., at 340 °C, when compared to the physical mixture. Similarly, in the later stage at 500 °C, the physical mixture underwent weight loss of almost 95%, while the weight loss observed in inclusion complexes was 10−13% lower than that of the physical mixture. These results indicated that the inclusion of OOSS dye into the hydrophobic cavity of β-CD enhanced thermal stability. Inclusion complexes showed lower degradation at the initial stage as well as at the later stage when compared with pure β-CD, OOSS dye, and their physical mixture. These findings are in good agreement with the inclusion of OOSS dye in the β-CD cavity and confirm complexation.[56−59]

DSC thermograms of β-CD, OOSS dye, physical mixture, and inclusion complexes are shown in Figure 5. A broad

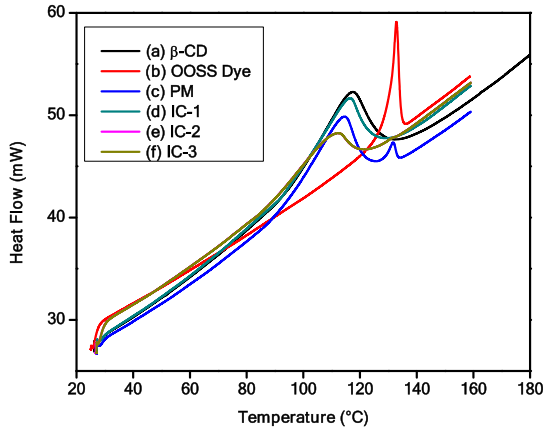

Figure 5. Differential scanning calorimetric (DSC) thermogram of (a) β-CD, (b) OOSS dye, (c) physical mixture, (d) IC-1, (e) IC-2, and (f) IC-3.

endothermic peak observed at 80−120 °C was presented by β-CD, which could be due to the liberation of water molecules from the β-CD cavity,[60] while the OOSS dye displayed a characteristic sharp peak at 132 °C. The physical mixture, however, showed two peaks, i.e., the similar characteristic peaks of β-CD and the OOSS dye, indicating that there was no interaction between β-CD and the OOSS dye. The appearance of two peaks attributed to the physical property was similar to that for the pure β-CD and OOSS dye, and the sample was just a mixture of β-CD and OOSS dye.[61] The DSC curves of the inclusion complexes displayed a completely different pattern when compared with β-CD, OOSS dye, and their physical mixture. The absence of the melting endotherm of the OOSS dye at 132 °C and a less pronounced peak with a slight shift where pure β-CD occurred confirmed an interaction between β-CD and the OOSS dye.[55] In addition, the peak occurring in inclusion complexes (IC-1 and IC-2) shifted slightly and reduced in intensity on increasing the concentration of the OOSS dye, indicating the substitution of crystal water with the OOSS dye from the cavity. This suggests that the hydrophobic OOSS dye has greater affinity with the hydrophobic cavity of β-CD than water. The characteristic peaks of IC-2 and IC-3 are almost identical, which is attributed to the saturation of OOSS dye inside the cavity. These findings are in good agreement with the inclusion of OOSS dye in the β-CD cavity and confirm complexation.

The crystal behavior of cyclodextrin inclusion complexes was analyzed by XRD. Figure 6 displays the XRD patterns of β-CD, OOSS dye, physical mixture, and its inclusion complexes. As can be seen in Figure 6a, the XRD pattern of β-CD displayed many crystalline peaks at 4.6, 9.1, 10.8, 12.6, 14.8, 17.2, 19.7, and 22.8°, indicating the crystalline nature of β-CD, which is in good agreement with the reported literature.[62,63] The intense diffraction peaks of β-CD at lower 2θ values and minor signatures at higher 2θ are the characteristics of a "cage-type"

https://dx.doi.org/10.1021/acsomega.0c05684
ACS Omega 2021, 6, 4776−4782

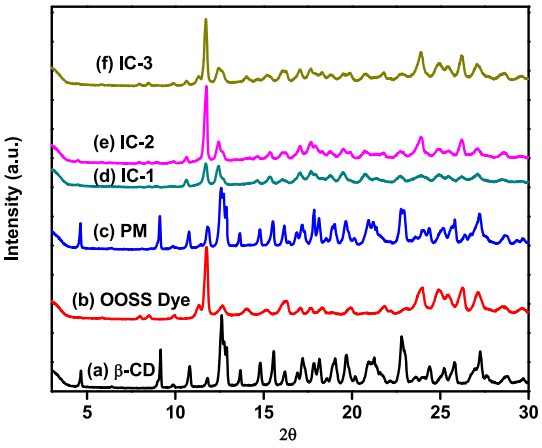

Figure 6. X-ray diffraction (XRD) patterns of (a) β-CD, (b) OOSS dye, (c) physical mixture, (d) IC-1, (e) IC-2, and (f) IC-3.

crystalline structure.[64] Figure 6b displays the XRD pattern of the OOSS dye, which exhibits major peaks at 2θ = 11.7, 16.2, 24, 24.9, 26.2, and 27.1°. Figure 6c displays the XRD pattern of the physical mixture, which shows characteristic peaks of β-CD, i.e., 2θ = 4.6, 9.1, 10.8, 12.6, and 22.8°, and the OOSS dye, i.e., 2θ = 11.7, 16.2, 24, and 27.1°, with a slight decrease in intensity. These results show that the physical mixture is a simple superimposition of β-CD and the OOSS dye. Figure 6d–f shows the XRD patterns of IC-1, IC-2, and IC-3, respectively. The lines of evidence for the inclusion complex formation are (i) disappearance of peaks, (ii) the formation of diffused peaks, and (iii) the appearance of new peaks.[65] The XRD patterns of all of the three inclusion complexes seem very different from those of the physical mixture, and most of the crystalline diffraction peaks disappear after complexation.[66] The new characteristic peaks of IC-1 occur at 2θ = 15.3, 18.7, and 20.7° with lower intensity. A similar phenomenon can be observed in IC-2 and IC-3 with intensity appeared to be increased as a function of concentration. In IC-2, the new characteristic peaks appear at 2θ = 15.3, 18.7, and 20.7°. In IC-3, the new characteristic peaks appear at 2θ = 15.2, 18.7, and 20.8°. It is well known that the peak at 2θ = ~20° in cyclodextrin inclusion complexes is a characteristic of "channel-type" packaging from cage-type packaging, which is formed only when an appropriate guest molecule is incorporated.[67] These findings indicate that the complexation of β-CD with the OOSS dye reoriented the β-CD molecule due to which most of the crystalline β-CD peaks disappeared and showed strong evidence of the inclusion complex formation.

4. CONCLUSIONS

In summary, we demonstrated that the highly toxic OOSS dye could be removed from aqueous solution by inclusion complex formation between β-CD and the OOSS dye. The formation of host–guest complexes via the coprecipitation method was driven by hydrophobic–hydrophobic interactions. The effect of various concentrations of OOSS dye showed that on increasing the concentration of OOSS dye, the stability of the inclusion complex further enhanced. Our results demonstrated that the hydrophobic OOSS dye showed greater affinity to the hydrophobic cavity of β-CD when compared to the hydrophilic crystal violet dye. The effective competitive complexation was evidenced by UV–vis spectroscopy. It was also noticed that the stability of the OOSS dye improved after complexation with β-CD. β-CD also exhibited excellent potential for water purification and can play a significant role in removing the highly toxic OOSS dye from the industrial effluent. It could be expected that the reported cost-effective and straightforward strategy could be utilized for removing other azo dyes.

■ ASSOCIATED CONTENT

Supporting Information

The Supporting Information is available free of charge at https://pubs.acs.org/doi/10.1021/acsomega.0c05684.

Formation of inclusion complex of the OOSS dye with β-CD in (a) industrial water (b) and lake water (PDF)

■ AUTHOR INFORMATION

Corresponding Author

Kamlesh Kumar – *CSIR-Central Scientific Instruments Organisation, Chandigarh 160030, India; Academy of Scientific and Innovative Research (AcSIR), Ghaziabad 201002, India;* orcid.org/0000-0003-1799-1421; Email: kamlesh.kumar@csio.res.in

Authors

Anas Saifi – *CSIR-Central Scientific Instruments Organisation, Chandigarh 160030, India; Academy of Scientific and Innovative Research (AcSIR), Ghaziabad 201002, India*

Jojo P. Joseph – *Institute of Nano Science and Technology, Mohali 160062, Punjab, India*

Atul Pratap Singh – *Department of Chemistry, Chandigarh University, Mohali 140413, Punjab, India*

Asish Pal – *Institute of Nano Science and Technology, Mohali 160062, Punjab, India;* orcid.org/0000-0002-6158-1158

Complete contact information is available at: https://pubs.acs.org/10.1021/acsomega.0c05684

Notes

The authors declare no competing financial interest.

■ ACKNOWLEDGMENTS

This research was funded by SERB-DST (SRG/2019/001628) and CSIR (MLP-2006).

■ REFERENCES

(1) Afkhami, A.; Moosavi, R. Adsorptive removal of Congo red, a carcinogenic textile dye, from aqueous solutions by maghemite nanoparticles. *J. Hazard. Mater.* **2010**, *174*, 398–403.

(2) Chatterjee, S.; Guha, N.; Krishnan, S.; Singh, A. K.; Mathur, P.; Rai, D. K. Selective and Recyclable Congo Red Dye Adsorption by Spherical Fe_3O_4 Nanoparticles Functionalized with 1,2,4,5-Benzenetetracarboxylic Acid. *Sci. Rep.* **2020**, *10*, No. 111.

(3) Hai, F. I.; Yamamoto, K.; Fukushi, K. Hybrid Treatment Systems for Dye Wastewater. *Crit. Rev. Environ. Sci. Technol.* **2007**, *37*, 315–377.

(4) Pereira, L.; Alves, M. Dyes—Environmental Impact and Remediation. In *Environmental Protection Strategies for Sustainable Development*; Malik, A.; Grohmann, E., Eds.; Springer Netherlands: Dordrecht, 2012; pp 111–162.

(5) Dye and Dye Intermediates. In *Van Nostrand's Scientific Encyclopedia*, 2006,.

(6) Cao, J.; Wei, L.; Huang, Q.; Wang, L.; Han, S. Reducing degradation of azo dye by zero-valent iron in aqueous solution. *Chemosphere* **1999**, *38*, 565–571.

https://dx.doi.org/10.1021/acsomega.0c05684
ACS Omega 2021, 6, 4776–4782

(7) Chen, M.; Ding, W.; Wang, J.; Diao, G. Removal of Azo Dyes from Water by Combined Techniques of Adsorption, Desorption, and Electrolysis Based on a Supramolecular Sorbent. *Ind. Eng. Chem. Res.* **2013**, *52*, 2403−2411.
(8) Cisneros, R. L.; Espinoza, A. G.; Litter, M. I. Photodegradation of an azo dye of the textile industry. *Chemosphere* **2002**, *48*, 393−399.
(9) Wu, J.-M.; Wen, W. Catalyzed Degradation of Azo Dyes under Ambient Conditions. *Environ. Sci. Technol.* **2010**, *44*, 9123−9127.
(10) Zhang, Y.; Bian, Y.; Niu, H.; Wang, Y.; Li, Y. Synthesis of colorant-modified polystyrene copolymers with tailored structures for toner applications. *RSC Adv.* **2016**, *6*, 104407−104415.
(11) Ahmad, A.; Mohd-Setapar, S. H.; Chuong, C. S.; Khatoon, A.; Wani, W. A.; Kumar, R.; Rafatullah, M. Recent advances in new generation dye removal technologies: novel search for approaches to reprocess wastewater. *RSC Adv.* **2015**, *5*, 30801−30818.
(12) Gu, F.; Geng, J.; Li, M.; Chang, J.; Cui, Y. Synthesis of Chitosan−Ignosulfonate Composite as an Adsorbent for Dyes and Metal Ions Removal from Wastewater. *ACS Omega* **2019**, *4*, 21421−21430.
(13) Lee, K. E.; Morad, N.; Teng, T. T.; Poh, B. T. Reactive Dye Removal Using Inorganic−Organic Composite Material: Kinetics, Mechanism, and Optimization. *J. Dispersion Sci. Technol.* **2014**, *35*, 1557−1570.
(14) Manippady, S. R.; Singh, A.; Basavaraja, B. M.; Samal, A. K.; Srivastava, S.; Saxena, M. Iron−Carbon Hybrid Magnetic Nanosheets for Adsorption-Removal of Organic Dyes and 4-Nitrophenol from Aqueous Solution. *ACS Appl. Nano Mater.* **2020**, *3*, 1571−1582.
(15) Vattikuti, S. V. P.; Reddy, P. A. K.; Shim, J.; Byon, C. Visible-Light-Driven Photocatalytic Activity of SnO_2−ZnO Quantum Dots Anchored on g-C_3N_4 Nanosheets for Photocatalytic Pollutant Degradation and H_2 Production. *ACS Omega* **2018**, *3*, 7587−7602.
(16) Zaghbani, N.; Hafiane, A.; Dhahbi, M. Removal of Safranin T from wastewater using micellar enhanced ultrafiltration. *Desalination* **2008**, *222*, 348−356.
(17) Lee, M.; Oh, S. Y.; Pathak, T. S.; Paeng, I. R.; Cho, B.-Y.; Paeng, K.-J. Selective solid-phase extraction of catecholamines by the chemically modified polymeric adsorbents with crown ether. *J. Chromatogr. A* **2007**, *1160*, 340−344.
(18) Chen, M.; Shang, T.; Fang, W.; Diao, G. Study on adsorption and desorption properties of the starch grafted p-tert-butyl-calix[n]-arene for butyl Rhodamine B solution. *J. Hazard. Mater.* **2011**, *185*, 914−921.
(19) Yilmaz, E.; Memon, S.; Yilmaz, M. Removal of direct azo dyes and aromatic amines from aqueous solutions using two β-cyclodextrin-based polymers. *J. Hazard. Mater.* **2010**, *174*, 592−597.
(20) Szejtli, J. Introduction and General Overview of Cyclodextrin Chemistry. *Chem. Rev.* **1998**, *98*, 1743−1754.
(21) Alsbaiee, A.; Smith, B. J.; Xiao, L.; Ling, Y.; Helbling, D. E.; Dichtel, W. R. Rapid removal of organic micropollutants from water by a porous β-cyclodextrin polymer. *Nature* **2016**, *529*, 190−194.
(22) Mohanty, J.; Bhasikuttan, A. C.; Nau, W. M.; Pal, H. Host−Guest Complexation of Neutral Red with Macrocyclic Host Molecules: Contrasting pKa Shifts and Binding Affinities for Cucurbit[7]uril and β-Cyclodextrin. *J. Phys. Chem. B* **2006**, *110*, 5132−5138.
(23) Ozmen, E. Y.; Sezgin, M.; Yilmaz, A.; Yilmaz, M. Synthesis of β-cyclodextrin and starch based polymers for sorption of azo dyes from aqueous solutions. *Bioresour. Technol.* **2008**, *99*, 526−531.
(24) Shaikh, M.; Mohanty, J.; Sundararajan, M.; Bhasikuttan, A. C.; Pal, H. Supramolecular Host−Guest Interactions of Oxazine-1 Dye with β- and γ-Cyclodextrins: A Photophysical and Quantum Chemical Study. *J. Phys. Chem. B* **2012**, *116*, 12450−12459.
(25) Yilmaz, A.; Yilmaz, E.; Yilmaz, M.; Bartsch, R. A. Removal of azo dyes from aqueous solutions using calix[4]arene and β-cyclodextrin. *Dyes Pigm.* **2007**, *74*, 54−59.
(26) Joseph, J. P.; Singh, A.; Gupta, D.; Miglani, C.; Pal, A. Tandem Interplay of the Host−Guest Interaction and Photoresponsive Supramolecular Polymerization to 1D and 2D Functional Peptide Materials. *ACS Appl. Mater. Interfaces* **2019**, *11*, 28213−28220.
(27) Consonni, R.; Recca, T.; Dettori, M. A.; Fabbri, D.; Delogu, G. Structural Characterization of Imazalil/β-Cyclodextrin Inclusion Complex. *J. Agric. Food Chem.* **2004**, *52*, 1590−1593.
(28) Paczkowska, M.; Mizera, M.; Szymanowska-Powałowska, D.; Lewandowska, K.; Błaszczak, W.; Gościańska, J.; Pietrzak, R.; Cielecka-Piontek, J. β-Cyclodextrin complexation as an effective drug delivery system for meropenem. *Eur. J. Pharm. Biopharm.* **2016**, *99*, 24−34.
(29) Numanoğlu, U.; Şen, T.; Tarimci, N.; Kartal, M.; Koo, O. M. Y.; Önyüksel, H. Use of cyclodextrins as a cosmetic delivery system for fragrance materials: Linalool and benzyl acetate. *AAPS PharmSciTech* **2007**, *8*, 34−42.
(30) Wang, Z.; Zhang, P.; Hu, F.; Zhao, Y.; Zhu, L. A crosslinked β-cyclodextrin polymer used for rapid removal of a broad-spectrum of organic micropollutants from water. *Carbohydr. Polym.* **2017**, *177*, 224−231.
(31) Zhao, H.-t.; Ma, S.; Zheng, S.-y.; Han, S.-w.; Yao, F.-x.; Wang, X.-z.; Wang, S.-s.; Feng, K. β−cyclodextrin functionalized biochars as novel sorbents for high-performance of Pb^{2+} removal. *J. Hazard. Mater.* **2019**, *362*, 206−213.
(32) Xie, Z.-W.; Lin, J.-C.; Xu, M.-Y.; Wang, H.-Y.; Wu, Y.-X.; He, F.-A.; Jiang, H.-L. Novel Fe_3O_4 Nanoparticle/β-Cyclodextrin-Based Polymer Composites for the Removal of Methylene Blue from Water. *Ind. Eng. Chem. Res.* **2020**, *59*, 12270−12281.
(33) Yuan, Z.; Liu, H.; Wu, H.; Wang, Y.; Liu, Q.; Wang, Y.; Lincoln, S. F.; Guo, X.; Wang, J. Cyclodextrin Hydrogels: Rapid Removal of Aromatic Micropollutants and Adsorption Mechanisms. *J. Chem. Eng. Data* **2020**, *65*, 678−689.
(34) Guo, R.; Liu, H.; Yang, K.; Wang, S.; Sun, P.; Gao, H.; Wang, B.; Chen, F. β-Cyclodextrin Polymerized in Cross-Flowing Channels of Biomass Sawdust for Rapid and Highly Efficient Pharmaceutical Pollutants Removal from Water. *ACS Appl. Mater. Interfaces* **2020**, *12*, 32817−32826.
(35) Hu, X.; Xu, G.; Zhang, H.; Li, M.; Tu, Y.; Xie, X.; Zhu, Y.; Jiang, L.; Zhu, X.; Ji, X.; Li, Y.; Li, A. Multifunctional β-Cyclodextrin Polymer for Simultaneous Removal of Natural Organic Matter and Organic Micropollutants and Detrimental Microorganisms from Water. *ACS Appl. Mater. Interfaces* **2020**, *12*, 12165−12175.
(36) Nasiri, J.; Motamedi, E.; Naghavi, M. R.; Ghafoori, M. Removal of crystal violet from water using β-cyclodextrin functionalized biogenic zero-valent iron nanoadsorbents synthesized via aqueous root extracts of *Ferula persica*. *J. Hazard. Mater.* **2019**, *367*, 325−338.
(37) Fan, L.; Zhang, Y.; Luo, C.; Lu, F.; Qiu, H.; Sun, M. Synthesis and characterization of magnetic β-cyclodextrin−chitosan nanoparticles as nano-adsorbents for removal of methyl blue. *Int. J. Biol. Macromol.* **2012**, *50*, 444−450.
(38) Crini, G.; Peindy, H. N. Adsorption of C.I. Basic Blue 9 on cyclodextrin-based material containing carboxylic groups. *Dyes Pigm.* **2006**, *70*, 204−211.
(39) Zhao, R.; Wang, Y.; Li, X.; Sun, B.; Wang, C. Synthesis of β-Cyclodextrin-Based Electrospun Nanofiber Membranes for Highly Efficient Adsorption and Separation of Methylene Blue. *ACS Appl. Mater. Interfaces* **2015**, *7*, 26649−26657.
(40) Duan, Z.; Wei, S.; Bian, H.; Guan, C.; Zhu, L.; Xia, D. Inclusion as an efficient purification method for specific removal of tricyclic organic sulfur/nitrogen pollutants in fuel and effluent with cyclodextrin polymers. *Sep. Purif. Technol.* **2021**, *254*, No. 117643.
(41) Chen, B.; Chen, S.; Zhao, H.; Liu, Y.; Long, F.; Pan, X. A versatile β-cyclodextrin and polyethyleneimine bi-functionalized magnetic nanoadsorbent for simultaneous capture of methyl orange and Pb(II) from complex wastewater. *Chemosphere* **2019**, *216*, 605−616.
(42) Qin, X.; Bai, L.; Tan, Y.; Li, L.; Song, F.; Wang, Y. β-Cyclodextrin-crosslinked polymeric adsorbent for simultaneous removal and stepwise recovery of organic dyes and heavy metal ions: Fabrication, performance and mechanisms. *Chem. Eng. J.* **2019**, *372*, 1007−1018.
(43) Arteshi, Y.; Aghanejad, A.; Davaran, S.; Omidi, Y. Semi self-doped electroconductive and biocompatible polyaniline/sulfonated β-

https://dx.doi.org/10.1021/acsomega.0c05684
ACS Omega 2021, 6, 4776−4782

cyclodextrin (PANI/SCD) inclusion complex with potential use in regenerative medicine. *Int. J. Polym. Mater. Polym. Biomater.* **2020**, *69*, 437−448.
(44) Zare, E. N.; Lakouraj, M. M.; Mohseni, M. Biodegradable polypyrrole/dextrin conductive nanocomposite: Synthesis, characterization, antioxidant and antibacterial activity. *Synth. Met.* **2014**, *187*, 9−16.
(45) Dandawate, P.; Vemuri, K.; Khan, E. M.; Sritharan, M.; Padhye, S. Synthesis, characterization and anti-tubercular activity of ferrocenyl hydrazones and their β-cyclodextrin conjugates. *Carbohydr. Polym.* **2014**, *108*, 135−144.
(46) Shan, X.; Jiang, K.; Li, J.; Song, Y.; Han, J.; Hu, Y. Preparation of beta-Cyclodextrin Inclusion Complex and Its Application as an Intumescent Flame Retardant for Epoxy. *Polymers* **2019**, *11*, No. 71.
(47) Hamdi, H.; Abderrahim, R.; Meganem, F. Spectroscopic studies of inclusion complex of β-cyclodextrin and benzidine diammonium dipicrate. *Spectrochim. Acta, Part A* **2010**, *75*, 32−36.
(48) Tang, B.; Chen, Z.-Z.; Zhang, N.; Zhang, J.; Wang, Y. Synthesis and characterization of a novel cross-linking complex of β-cyclodextrin-o-vanillin furfuralhydrazone and highly selective spectrofluorimetric determination of trace gallium. *Talanta* **2006**, *68*, 575−580.
(49) Kemelbekov, U.; Luo, Y.; Orynbekova, Z.; Rustembekov, Z.; Haag, R.; Saenger, W.; Praliyev, K. IR, UV and NMR studies of β-cyclodextrin inclusion complexes of kazcaine and prosidol bases. *J. Inclusion Phenom. Macrocyclic Chem.* **2011**, *69*, 181−190.
(50) Sambasevam, K. P.; Mohamad, S.; Sarih, N. M.; Ismail, N. A. Synthesis and Characterization of the Inclusion Complex of beta-cyclodextrin and Azomethine. *Int. J. Mol. Sci.* **2013**, *14*, 3671−3682.
(51) Wang, B.; He, J.; Sun, D.; Zhang, R.; Han, B.; Huang, Y.; Yang, G. Preparation of β-cyclodextrin−polyaniline complex in supercritical CO_2. *Eur. Polym. J.* **2005**, *41*, 2483−2487.
(52) Wang, H. Y.; Han, J.; Feng, X. G. Spectroscopic study of orange G−β-cyclodextrin complex and its analytical application. *Spectrochim. Acta, Part A* **2007**, *66*, 578−585.
(53) Zhu, S.; Zhao, F.; Deng, M.; Zhang, T.; Lü, C. Construction of β-cyclodextrin derived CDs-coupled block copolymer micelles loaded with CdSe/ZnS QDs via host-guest interaction for ratiometric fluorescence sensing of metal ions. *Dyes Pigm.* **2019**, *168*, 369−380.
(54) Bani-Yaseen, A. D.; Mo'ala, A. Spectral, thermal, and molecular modeling studies on the encapsulation of selected sulfonamide drugs in β-cyclodextrin nano-cavity. *Spectrochim. Acta, Part A* **2014**, *131*, 424−431.
(55) Kringel, D. H.; Antunes, M. D.; Klein, B.; Crizel, R. L.; Wagner, R.; de Oliveira, R. P.; Dias, A. R. G.; da Rosa Zavareze, E. Production, Characterization, and Stability of Orange or Eucalyptus Essential Oil/β-Cyclodextrin Inclusion Complex. *J. Food Sci.* **2017**, *82*, 2598−2605.
(56) Zhang, N.; Shen, J.; Pasquinelli, M. A.; Hinks, D.; Tonelli, A. E. Formation and characterization of an inclusion complex of triphenyl phosphate and β-cyclodextrin and its use as a flame retardant for polyethylene terephthalate. *Polym. Degrad. Stab.* **2015**, *120*, 244−250.
(57) Gao, S.; Jiang, J.-Y.; Liu, Y.-Y.; Fu, Y.; Zhao, L.-X.; Li, C.-Y.; Ye, F. Enhanced Solubility, Stability, and Herbicidal Activity of the Herbicide Diuron by Complex Formation with beta-Cyclodextrin. *Polymers* **2019**, *11*, No. 1396.
(58) Marcolino, V. A.; Zanin, G. M.; Durrant, L. R.; Benassi, M. D. T.; Matioli, G. Interaction of Curcumin and Bixin with β-Cyclodextrin: Complexation Methods, Stability, and Applications in Food. *J. Agric. Food Chem.* **2011**, *59*, 3348−3357.
(59) Menezes, P. P.; Serafini, M. R.; Santana, B. V.; Nunes, R. S.; Quintans, L. J.; Silva, G. F.; Medeiros, I. A.; Marchioro, M.; Fraga, B. P.; Santos, M. R. V.; Araújo, A. A. S. Solid-state β-cyclodextrin complexes containing geraniol. *Thermochim. Acta* **2012**, *548*, 45−50.
(60) Geng, Q.; Li, T.; Wang, X.; Chu, W.; Cai, M.; Xie, J.; Ni, H. The mechanism of bensulfuron-methyl complexation with β-cyclodextrin and 2-hydroxypropyl-β-cyclodextrin and effect on soil adsorption and bio-activity. *Sci. Rep.* **2019**, *9*, No. 1882.
(61) Xu, F.; Yang, Q.; Wu, L.; Qi, R.; Wu, Y.; Li, Y.; Tang, L.; Guo, D.-a.; Liu, B. Investigation of Inclusion Complex of Patchouli Alcohol with β-Cyclodextrin. *PLoS One* **2017**, *12*, No. e0169578.
(62) Ranganathan, P.; Mutharani, B.; Chen, S.-M.; Sireesha, P. Polystyrene:β-Cyclodextrin Inclusion Complex-Supported Y_2O_3-Based Electrochemical Sensor: Effective and Simultaneous Determination of 4-Aminoantipyrine and Acyclovir Drugs. *J. Phys. Chem. C* **2019**, *123*, 12211−12222.
(63) Trindade, G. G. G.; Thrivikraman, G.; Menezes, P. P.; França, C. M.; Lima, B. S.; Carvalho, Y. M. B. G.; Souza, E. P. B. S. S.; Duarte, M. C.; Shanmugam, S.; Quintans-Júnior, L. J.; Bezerra, D. P.; Bertassoni, L. E.; Araújo, A. A. S. Carvacrol/β-cyclodextrin inclusion complex inhibits cell proliferation and migration of prostate cancer cells. *Food Chem. Toxicol.* **2019**, *125*, 198−209.
(64) Al-Burtomani, S. K. S.; Suliman, F. O. Inclusion complexes of norepinephrine with β-cyclodextrin, 18-crown-6 and cucurbit[7]uril: experimental and molecular dynamics study. *RSC Adv.* **2017**, *7*, 9888−9901.
(65) Abarca, R. L.; Rodríguez, F. J.; Guarda, A.; Galotto, M. J.; Bruna, J. E. Characterization of beta-cyclodextrin inclusion complexes containing an essential oil component. *Food Chem.* **2016**, *196*, 968−975.
(66) Rocha, S.; de Lima, S. G.; Viana, B. C.; Costa, J. G. M.; Santos, F. E. P. Characterization of the inclusion complex of the essential oil of *Lantana camara* L. and β-cyclodextrin by vibrational spectroscopy, GC−MS, and X-ray diffraction. *J. Inclusion Phenom. Macrocyclic Chem.* **2018**, *91*, 95−104.
(67) Rusa, C. C.; Bullions, T. A.; Fox, J.; Porbeni, F. E.; Wang, X.; Tonelli, A. E. Inclusion Compound Formation with a New Columnar Cyclodextrin Host. *Langmuir* **2002**, *18*, 10016−10023.

https://dx.doi.org/10.1021/acsomega.0c05684
ACS Omega 2021, 6, 4776−4782